J. Fluid Mech. (1976), *vol.* 77, *part* 3, *pp.* 531–560
Printed in Great Britain

Sedimentological and fluid-dynamic implications of the turbulent bursting phenomenon in geophysical flows

By ROSCOE G. JACKSON

Department of Geological Sciences, Northwestern University, Evanston, Illinois 60201

(Received 10 November 1975)

The bursting process in turbulent boundary layers provides new insight on turbulence phenomena, mechanics of sedimentation, and genesis of bedforms in natural geophysical flows. Recent visualization experiments suggest that the turbulent boundary layer can be divided into an inner zone, whose essential characteristics scale with inner (wall) variables, and an outer zone, whose properties scale with the fluid-dynamic variables of the entire flow. The inner zone is distinguished by (i) a viscous sublayer displaying spanwise alternations of high- and low-speed streaks and (ii) episodic disruption by lift-ups of low-speed streaks. Oscillatory growth and breakup stages of the Stanford model of bursting characterize the turbulent structure of the outer zone. The burst cycle exists in turbulent boundary layers of all natural flows except perhaps (i) open-channel flows in the upper part of the upper flow regime and (ii) wind-generated surface waves.

Fluid motions described as kolks and boils in incompressible open-channel flows correspond to the *oscillatory growth stage and the late oscillatory growth* and breakup stages, respectively, of the Stanford model of bursting. Supporting evidence includes (i) close similarity of gross fluid motions, (ii) equivalent scaling of boils and bursts, and (iii) intensification of boils and bursts in adverse pressure gradients and over rough beds. McQuivey's (1973) turbulence measurements show that the Eulerian integral time scale T_E scales with the same outer variables as *boil* periodicity and burst periodicity. It is hypothesized that T_E equals the mean duration of bursts at a point in the flow.

Bedforms governed by the turbulent structure of the inner zone (microforms) cannot form if the sublayer is disrupted by bed roughness. The conditions for the existence of two common microforms and their spacings scale with the inner variables. Grain roughness increases the vertical intensity of the turbulence (by enhancing lift-ups) within the inner zone, thereby explaining textural differences between the coarse ripple and fine ripple bed stages of Moss (1972).

Mesoforms respond to the fluid-dynamical regime in the outer zone and scale with the outer variables. The mean spacing of dunelike large-scale ripples in equilibrium open-channel flows is proportional to the boundary-layer thickness and equals the length scale formed by the product of the free-stream velocity and the boil period.

Strong upward flow in a burst provides the vertical anisotropy in the turbulence which is needed to suspend sediment. Bursting promotes the entrainment of more and coarser sediment than tractive forces alone can accomplish.

1. Introduction

Successive experimental investigations of fluid motions in turbulent boundary layers have disclosed a complex quasi-ordered flow structure which consists of a deterministic sequence of fluid motions occurring randomly in space and in time (reviews in Laufer 1975; Offen & Kline 1975). Although the existence of this turbulent structure in natural fluid flows has been considered (Mollo-Christensen 1973; Gordon 1974, 1975*a*; Heathershaw 1974), the extent to which the structural features appear remains to be explored thoroughly. Possible relations between the turbulent structure and either the topographic features of the underlying erodible bed or the dispersion of sediment also remain neglected. The present paper attempts to remedy these shortcomings in the following manner: (i) demonstrating from several lines of indirect evidence that the turbulent structure exists in many natural flows, (ii) proposing several relationships between turbulent structure and bedforms of two fundamental kinds, and (iii) drawing some implications of the role of the turbulent structure in dispersal of sediment vertically throughout the boundary layer.

2. Structure of turbulent boundary layers in ideally simple flows

The turbulent structure of shallow subcritical incompressible flows over smooth rigid walls has been investigated by two visualization techniques. A bubble–dye technique developed at Stanford University has led to a structural model of the viscous sublayer which consists of a spanwise alternation of low-velocity and high-velocity streaks of fluid (Kline *et al.* 1967). The wall streaks display significant streamwise vorticity and appeared randomly in space and in time. More recent research at Stanford has produced a qualitative model of the structure of the transitional (buffer), logarithmic and outer (wake) regions of turbulent boundary layers. Individual low-speed streaks are postulated to lift up from the sublayer, oscillate rapidly and enlarge, and finally break up into chaotic motion. Figure 1 outlines the essential features of these three events, which collectively constitute the 'burst cycle' or 'bursting'.

Using a different visualization technique, investigators at Ohio State University constructed an alternative structural model of the turbulent boundary layer. Major components of this model are summarized in figure 2. All fluid motions sketched in figures 1 and 2 are relative to mean fluid velocity. In particular, reverse flow was never observed from a fixed frame of reference (Nychas, Hershey & Brodkey 1973; Offen & Kline 1975, p. 211).

There are many similarities in the two structural models outlined above (Offen & Kline 1975). Both consider the turbulent boundary layer to be a composite of two very different zones (figures 1(*f*) and 2(*e*)). The boundary between zones is located differently in each model but coincides roughly with the boundary between the transition and logarithmic regions of the conventional turbulent boundary layer. The inner zone of both models is distinguished by (i) being the site of most of the production of turbulence in the boundary layer, (ii) its innermost layer, the viscous sublayer, showing a periodically disrupted

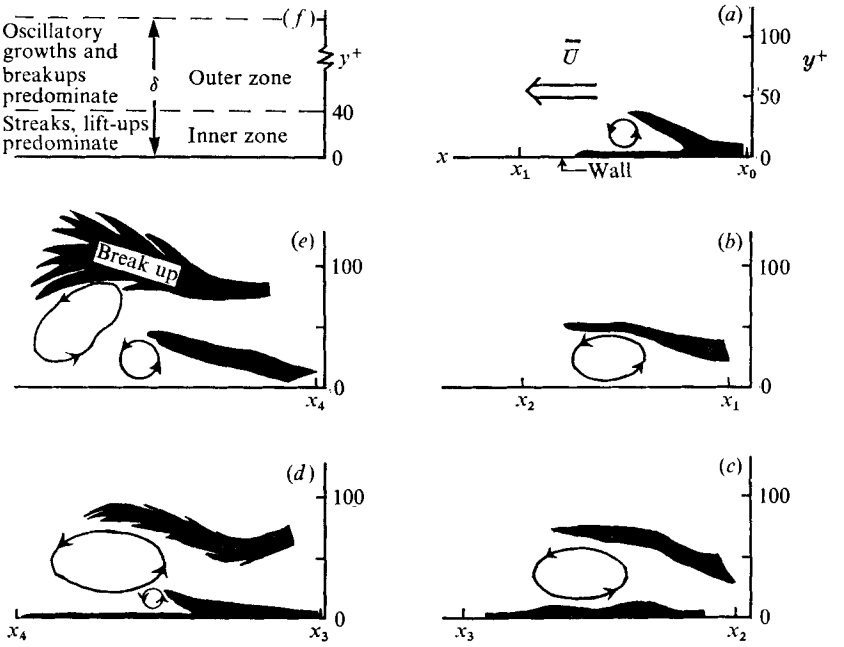

FIGURE 1. Structure of the turbulent boundary layer revealed by bubble–dye visualization technique. (*a*)–(*e*) sketch sequential events of the burst cycle from advected view of mean flow. (*a*) Lift-up of low-speed wall streak to initiate burst; the vortex is associated with the local advected separation bubble (separation only in frame of reference of mean flow). (*b*) Oscillatory growth of lifted wall streak. (*c*) Continued growth of lifted wall streak, with passage over next low-speed wall streak downstream. (*d*) Early phase of breakup of burst, which starts lift-up of underlying wall streak [cf. (*a*)]. (*e*) Termination of breakup and of first burst; breakup forms a large irregular vortex in front of lift-up of next burst downstream. (*f*) The structural regions of a turbulent boundary layer proposed by Kim *et al.* (1971) and Offen & Kline (1974). (*a*)–(*e*) are adapted from Offen & Kline (1973, figure 5.1; 1975, figure 1).

structure of spanwise alternating streaks of low- and high-speed fluid, and (iii) lift-up of low-speed wall streaks being induced by transverse vortices in areas of high local shear near the boundary between the two zones. The outer zones of both models have several features in common: (i) they are the sources of accelerated fluid moving towards the wall that precedes and probably initiates a burst, (ii) they contain large vortices near the breakup of the burst cycle, (iii) they contain downstream sweeps of low-speed ejections which penetrate and strongly interact with them, and (iv) the diameters of vortices forming in them often exceed half the local thickness of the boundary layer.

The visualization studies leave little doubt that events of the burst cycle constitute a dominant mechanism of fluid transfer in turbulent boundary layers. Instantaneous contributions from individual events such as sweeps, vortices and lift-ups to the various turbulence intensities are often many times the contribution from the background flow (Grass 1971; Kim, Kline & Reynolds 1971; Nychas *et al.* 1973). Probe measurements verify the large contributions made by

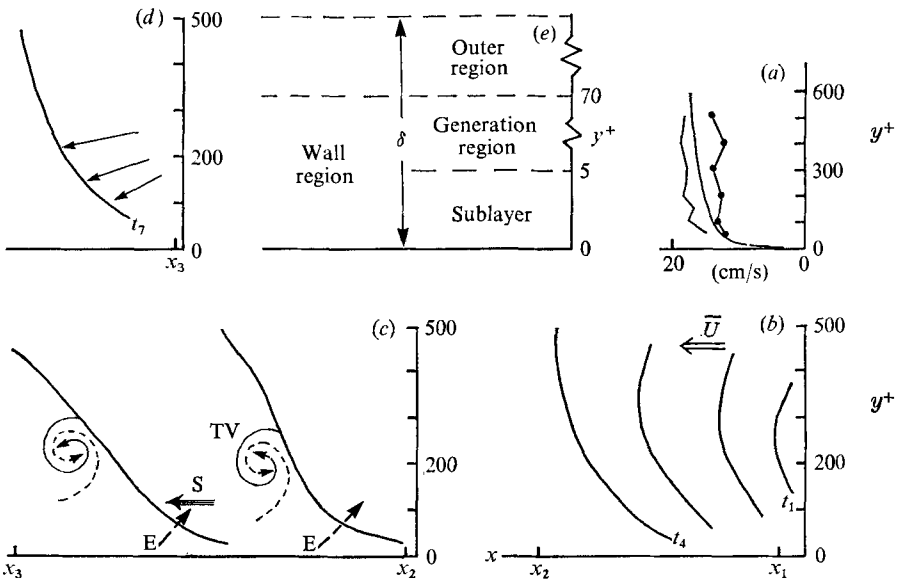

FIGURE 2. Structure of the turbulent boundary layer revealed by colloidal-particle visualization technique. (*a*) Typical profiles of the streamwise velocity of accelerated fluid (segmented solid line), mean flow (smooth solid line), and decelerated fluid (broken line with dots). (*b*)–(*d*) show sequential events of the burst cycle from advected view of mean flow. Each curved heavy line in (*b*) and (*c*) is an interface between accelerated fluid upstream and decelerated fluid. (*b*) Overall deceleration of fluid; then (starting at time t_1) progressive displacement by accelerated fluid. (*c*) Formation of transverse vortices (TV) just ahead of advancing interface. Ejection (E) of low-speed fluid from generation region interacts with accelerated fluid and is swept downstream as a 'sweep' (S). (*d*) Large-scale inflow terminates burst. Curved solid line is interface at time t_7 between accelerated fluid downstream and inflow. (*e*) Structural regions of the turbulent boundary layer proposed by Corino & Brodkey (1969). (*a*)–(*c*) are adapted from figures 6, 4 and 8, respectively, of Nychas *et al.* (1973), in whose experiments $\delta^+ \simeq 420$.

bursting to the production of turbulence (Kim *et al.* 1971; Wallace, Eckelmann & Brodkey 1972; Willmarth & Lu 1972, 1974; Gordon 1974, 1975*a*; Heathershaw 1974).

The experimental studies also disclosed scaling relations for turbulent boundary layers. An 'inner' law scales the average spacing of the sublayer streaks of the inner zone by using two wall variables

$$\lambda_s u_*/\nu \equiv \lambda_s^+ \simeq 100, \tag{1}$$

where λ_s is the average spanwise spacing of low-speed wall streaks, u_* the shear velocity and ν kinematic viscosity. λ_s^+ is a dimensionless expression in inner variables. Kline *et al.* (1967) proposed this empirical equation; they and subsequent investigators have verified it in many laboratory flows. A dimensionally identical equation has long been used to define the thickness δ_s of the viscous sublayer (Schlichting 1968, p. 568):

$$\delta_s u_*/\nu \equiv \delta_s^+ \simeq A, \tag{2}$$

where A is a dimensionless constant whose value ranges from 5 to 11·6. It

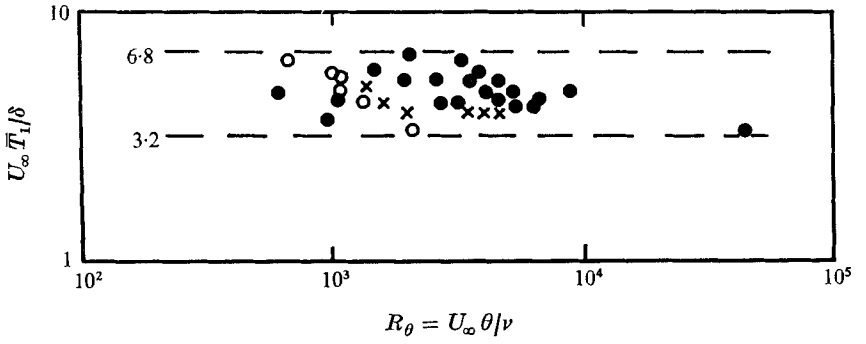

FIGURE 3. Scaling of burst periodicity with outer variables. Dashed lines define bandwidth of 2·1 which includes all data. ●, hot-wire air data; ×, hot-film water data; ○, visual water data. Data sources are Rao *et al.* (1971, figure 9) and Blinco & Simons (1975, figure 8).

has likewise long been appreciated that the viscous sublayer is disrupted whenever the bed roughness exceeds the sublayer thickness, according to

$$du_*/\nu \equiv d^+ > \delta_s^+, \tag{3}$$

where d is the diameter of the sedimentary particles. When d^+ reaches about 70, the viscous sublayer is disrupted completely and ceases to exist as a region definable from velocity profiles. Roughness elements in such flows penetrate the total thickness of the inner zone (figures 1 (*f*) and 2 (*e*)) and break up the organized pattern of sublayer streaks (Grass 1971).

The turbulent structure of the outer zone is dominated by the bursting process and is largely independent of the wall structure. Rao, Narasimha & Badri Narayanan (1971) proposed the following scaling relation for bursts in the outer zone:

$$U_\infty \bar{T}_1/\delta \equiv \bar{T}_1^* \simeq 5, \tag{4}$$

where $\bar{T}_1$ is the mean periodicity of bursts at a point in the flow, U_∞ is the free-stream velocity, and δ is the boundary-layer thickness. Laboratory measurements of burst periodicity (figure 3) show $\bar{T}_1^*$ to lie between 3 and 7 over the narrow range of momentum-thickness Reynolds numbers considered thus far. A constant value of 5 fits the data well and can be predicted from the Blasius resistance formula for flow Reynolds numbers R_∞ ($= U_\infty \delta/\nu$) of the order of 10^5 over smooth beds (Laufer & Badri Narayanan 1971). Burst frequency thus scales with the gross-flow variables U_∞ and δ, which makes (4) an 'outer' law.

3. Generalization of turbulent structure to geophysical flows

The visualization experiments from which the two-zone structural model was constructed employed ideally simple flows and boundary conditions. The flows were subcritical, steady, quasi-uniform, free of sedimentary particles, incompressible, and much less than one metre deep. The solid boundary was flat, hydraulically smooth and stationary. Natural flows rarely satisfy more than a few of these conditions. One must therefore evaluate to what extent the non-ideal

characteristics of natural flows may modify the turbulent structure observed in the laboratory.

Using the hydrogen-bubble technique, Grass (1971) observed wall streaks only in flows over a smooth bed. The elongated, sinuous streamwise vortices defining wall streaks were much less conspicuous over a hydraulically transitional bed and a rough bed. His figure 8 shows a gradual lift-up of low-speed streaks only in the smooth-bed flow. Flow over the rough boundary displayed sudden violent ejections of fluid from the interstices of large grains. Energetic events resembling oscillatory growth and breakup appeared over all three bed roughnesses. Grain roughness apparently disrupted the inner-zone structure but left the outer zone comparatively intact.

From standard velocity measurements, mostly the hot-wire anemometry thought by Offen & Kline (1974) to be incapable of discriminating events of the burst cycle, Gupta, Laufer & Badri Narayanan (1971), Laufer & Badri Narayanan (1971), Rao *et al.* (1971) and Lu & Willmarth (1973) have identified bursts in air flows through laboratory ducts. However, they could not detect individual stages of the burst cycle. Analysis of the turbulent structure of the outer region of the planetary boundary layer is complicated by convectional instabilities which can occur on time scales of the order of the burst periods predicted by (4). For example, Kaimal & Businger (1970) reported 'bursts' of high Reynolds stress which were produced by a convective plume and by a 'dust devil'. Haugen, Kaimal & Bradley (1971), Latham & Miksad (1974) and Markson (1975) attributed similar 'bursts' to other convectional phenomena. None of the limited data on 'bursting' periods in these papers follows (4).

The lower part (surface layer) of the planetary boundary layer shares several velocity features with incompressible turbulent boundary layers (Monin 1970, pp. 229–230; Panofsky 1974, pp. 147–156). In addition, Merceret (1972) has detected 'bursts' in velocity over a ploughed field and attributed them to the bursting process. If possible effects of convectional instabilities are disregarded, this evidence and the laboratory measurements favour a bursting model for air flows the same as the model used for incompressible flows (figures 1 and 2).

Scattered published results suggest that the structural model does not depend upon boundary-layer thickness. Other factors being equal, the inner-zone structure should remain much the same, because it scales independently of boundary-layer thickness. McQuivey's (1973, tables 9–12) measurements of streamwise turbulence intensity in outer zones of deep alluvial flows scale favourable with laboratory measurements by Laufer (1954, figure 5), Grass (1971, figure 5), Kim *et al.* (1971, figure 17) and McQuivey (1973, tables 1–6), suggesting a preservation of similarity. Time-series measurements of instantaneous fluid velocities and of Reynolds stresses in tidal currents of the Irish Sea (Heathershaw 1974) and in a tidal estuary (Gordon 1974, 1975*a*) revealed intermittent periods of intense momentum transport which both authors interpreted as the passage of bursts and sweeps across the current meter. Flow depths ranged from 8 m to 60 m. Mean periods between bursts appeared to scale according to (4), unlike the convectional momentum-transporting events reported from the planetary boundary layer.

The modification of the burst cycle by the introduction of mobile sediment is poorly understood. Many authors report a dampening of turbulence by increasing concentrations of suspended sediment (Matthes 1947, p. 261; Bagnold 1956, p. 265; Hampton 1972, pp. 790–791), but possible effects on turbulent structure remain undocumented. Yalin (1972, pp. 185–187) argued that suspended load reduces the length macroscales of turbulence but negligibly decreases turbulence intensities. The situation is little clearer for bed load. The turbulent structure almost certainly is modified when transfer of solid particles by grain-to-grain collisions prevails near the bed (Bagnold 1956, 1966, 1973). Turbulent properties of flows in which sediment is transported primarily by fluid shear probably differ little from those of single-phase flows, but relevant measurements to decide this question are lacking.

Unsteady flows present other complications. All non-oscillatory natural flows vary sufficiently slowly for the mean values of flow parameters to remain sensibly constant during each burst and during the time scale of the largest turbulent eddies. The burst cycle thus might change in magnitude or in frequency with time, because of different boundary-layer thicknesses or changing bed roughnesses, but flow unsteadiness *per se* would not modify the cycle. The same conclusion applies to slowly oscillating flows whose periods far exceed turbulent time scales. Examples of such flows are tidal currents, tsunamis, seiches and internal waves. No turbulence measurements to date imply any difference in turbulent properties between steady flows and these two classes of unsteady flows or between uniform flows and non-uniform flows (Bowden 1962; McQuivey 1973; Gordon 1974, 1975*a*, *b*; Heathershaw 1974).

On the other hand, the writer knows of no measurements of the burst cycle in the thin boundary layers beneath wind-generated shoaling waves. The swiftly reversing flow virtually precludes rational measurement, especially in view of the formation of vortices and of sudden jets in laminar wave boundary layers (Sleath 1970, 1974*a*, *b*). The extreme unsteadiness of U_∞ in at least those wave boundary layers with a small superimposed mean flow prohibits any objective use of (4) to estimate burst periods. Equation (4) is compromised further by the difficulty in defining boundary-layer thickness in such flows (Teleki 1972, p. 36). Finally, conditions governing transition from laminar to turbulent flow in wave boundary layers are not well established (Komar & Miller 1973, pp. 1105–1109; Sleath 1974*a*, pp. 302–303). These considerations demand extreme caution in extending the bursting process to wave boundary layers.

The problem of surface gravity waves also arises in other free-surface flows, which in the visualization experiments were in the lower flow regime of Simons, Richardson & Nordin (1965). Surface waves of upper-regime open-channel flows probably disrupt boundary-layer structure only when they break. The remarkably energetic large-scale turbulence of breaking antidunes and of chutes and pools (Simons *et al.* 1965, pp. 40–42; Guy, Simons & Richardson 1966) must overwhelm the less vigorous turbulent structure of bursting. The burst cycle is probably neither recognizable in nor relevant to such flows.

4. New evidence of bursting in alluvial flows

Previous attempts to recognize bursts in natural flows have relied on measurements of streamwise and vertical components of fluid velocity. These data have been interpreted to indicate the presence of bursts and sweeps (Gordon 1974, 1975*a*; Heathershaw 1974). However, no additional evidence has been offered to document the nature of bursting in these flows. Furthermore, any possible relation of the bursting process to conventional macroscales of turbulence theory remains unclear.

Visual evidence of bursts in alluvial flows

Observers since at least the time of Mark Twain (Clemens 1896, pp. 44–48) have reported distinctive patterns of turbulent fluid motions on the water surface of rivers. During a programme of hydraulic surveys of the lower Wabash River near Grayville, Illinois, Jackson (1975*a*, pp. 239–242) identified three types of water-surface macroturbulence phenomena recognized by Matthes (1947). One type, the well-known 'boil' (figure 4 and figure 5, plate 1), appeared to be a surface manifestation of bursting.

The fluid motions associated with boils have been discussed by Matthes (1947, figure 1), Znamenskaya (1963, p. 267 and panel II of figure 5) and Coleman (1969, pp. 198–206). Boils in the lower Wabash River could appear anywhere on the water surface but were largest and most energetic immediately downstream from crests of dunelike large-scale ripples (figure 5), particularly the transverse bars of Jackson (1976). The largest boils attained diameters of 2–4 m, raised the water surface by up to 10 cm, and persisted for as long as 20 s. Boil size was roughly proportional to depth (cf. figure 10 below).

Boils correspond to type III(1) macroturbulence phenomena of Matthes (1947), to 'local bulging of flow' of Znamenskaya (1963, p. 267), to 'structural eddy formations' of Korchokha (1968, pp. 555–556), and to 'boils' of Coleman (1969, figure 35A). Comparison of figure 4 with the appropriate descriptions in these four references reveals a close similarity in gross fluid motions, which suggests that all involve the same macroturbulence phenomenon.

Subsurface fluid motions responsible for boils could not be seen in the lower Wabash River because of water turbidity but it is likely that they were the upward-tilted streamwise vortices referred to as 'kolks' by Matthes (1947, figure 1 and table 1) and as 'longitudinal-vertical eddies' by Znamenskaya (1963, p. 267). Both authors described boils as the manifestation of upward-tilted vortices which reached the water surface.

Figure 6 proposes a time-sequential relation between boils and kolks and stages of the Stanford bursting model. The bed configuration and fluid motions are almost identical to those in Matthes (1947, figure 1).

Many lines of evidence support the hypothesis of figure 6. Perhaps the most compelling support comes from a comparison of fluid motions in bursts (figure 1) with fluid motions in boils and kolks (figures 4 and 5). The vigorous upward flow in boils and kolks resembles the powerful upward velocities observed during oscillatory growth stages by Kim *et al.* (1971) and by Offen & Kline (1973, 1974).

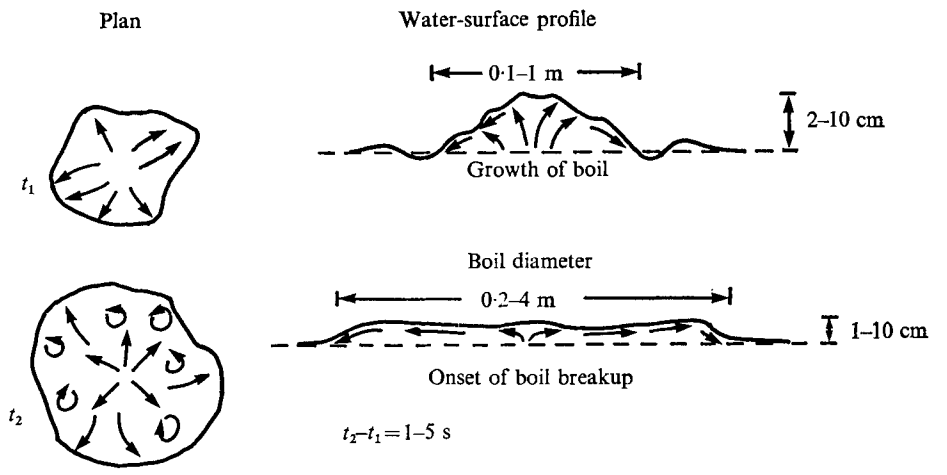

FIGURE 4. Development of typical boil in lower Wabash River. The view is that of an observer travelling with mean velocity of surface flow.

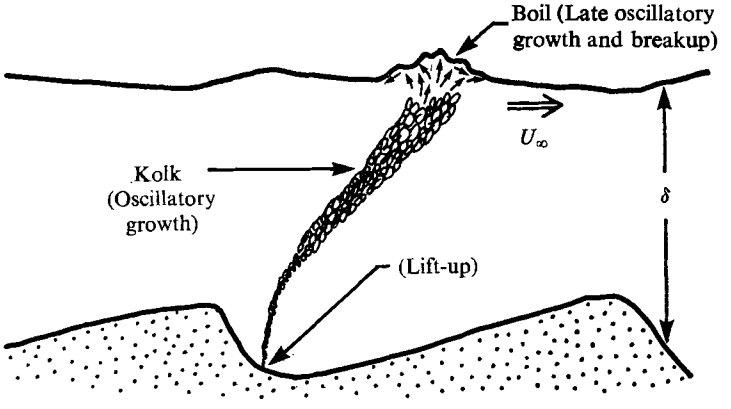

FIGURE 6. Postulated relation of boils and kolks to stages of the Stanford model of the bursting process. The relation also exists over flat beds. The fluid motions are in a time sequence which corresponds to figures 1 (*a*)–(*e*).

The longitudinal component of fluid velocity in a boil is significantly less (perhaps by 10–30%) than the mean ambient flow, which fact, for bursts, is amply documented in the laboratory investigations reviewed in § 2. Both boils and bursts are slowly rotating structures which appear randomly in space and in time. Only Matthes (1947, p. 258) reported a strong circulation in kolks (and then only near the bed). The dissipation stage of boils (figure 4) contains small (of the order of one tenth of the boil diameter) vortices with near-vertical axes; it would seem to correspond closely to the chaotic motion during breakup of a burst (figure 1 (*e*)). Finally, Grass (1971, p. 253) specifically attributed 'boils of fluid' on the water surface of his laboratory flow to the interaction of ejections (bursts) with the water surface.

A second argument for the process shown in figure 6 concerns effects of bed

roughness upon boil development. Although Matthes (1947), Znamenskaya (1963) and Korchokha (1968) described only boils which appeared over large-scale ripples, Coleman (1969, figure 37) observed boils over large-scale lineations whose long axes were parallel to the mean flow, under upper-regime flow in the Brahmaputra River. Boils in the lower Wabash River occurred over flat beds during strong lower-regime flows and over the flood plain during floods. Boils over flat beds, which were relatively coarse grained (mean size typically 2 mm), were less vigorous than their counterparts in equal depths over strongly rippled beds, although the boil frequency was not noticeably different when scaled by (4). Boils over the flood plain developed over ploughed ground and over corn stubble, each of which gives a substantial bottom roughness not present in the flat beds of channel flow. Flood-plain boils were exceedingly energetic and somewhat larger than other boils in the same flow depths. These observations point to an enhancement of the vigour and size of boils by bed roughness. This conclusion compares favourably with Grass's (1971, pp. 252–253) comment that ejections (bursts) became more violent with increased bed roughness.

Large-scale ripples constitute a form roughness which influences the development of kolks and boils. The observations of Matthes, Znamenskaya, Korchokha and Coleman demonstrate the tendency of boils to concentrate immediately downstream from the crestlines of large-scale ripples. Matthes, Znamenskaya and Korchokha also reported a preferential formation of kolks on lower slipfaces and troughs of large-scale ripples. The significant relation to bursting stems from Raudkivi's (1963, figure 4; 1966, figure 3) and Vanoni & Hwang's (1967, figure 4) measurements of uniformly adverse pressure gradients at the bed over leesides of artificial ripples. It is precisely in such unfavourable pressure gradients that bursts in laboratory flows are most energetic and frequent (Kline *et al.* 1967, p. 759 and figure 16(*b*)). In the Brahmaputra River, this localization of boils was sufficient for Coleman (1969, figures 32 and 34) to map boil patterns from aerial photographs; the patterns corresponded closely to sites of ripple crestlines.

A third line of evidence, somewhat tenuous, concerns measurements of longitudinal and vertical components of fluid velocity. Laboratory data of Grass (1971, pp. 249–250), Lu & Willmarth (1973, figure 14) and Brodkey, Wallace & Eckelmann (1974, p. 216) indicate a significantly greater contribution to Reynolds stress from burstlike events than from sweeplike events, in the outer zone of turbulent boundary layers. These results are in accord with the total absence of published reports of sweeplike turbulence phenomena in natural streams. Unhappily for the sake of this argument, however, Gordon's (1974, 1975*a*) data from a tidal flow showed a much less substantial difference (about 10%) between the Reynolds-stress contributions from burstlike events and those from sweeplike events.

If boils and kolks correspond to oscillatory growth and breakup events of bursting, then the frequency of appearance of boils at a point on the water surface should scale according to (4). Mean boil periodicity at a point on the water surface $\overline{T}_2$ in at least two streams scales (figure 7) as

$$U_\infty \overline{T}_2/\delta \equiv \overline{T}_2^* \simeq 7{\cdot}6. \tag{5}$$

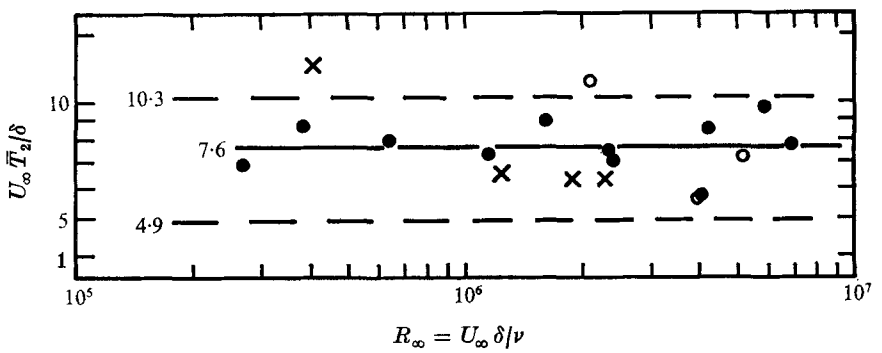

FIGURE 7. Scaling of mean periodicity of boils at a point on the water surface with outer variables. ○, lower Wabash River (14 September 1974); ●, lower Wabash River (9 November 1974); ×, Polomet' River. The two dashed lines define bandwidth of 2·1, which contains all but two points. Table 1 summarizes boil measurements.

Date	δ (m)	U_∞ (m/s)	$\bar{T}_2$ (s)	σ (s)	$U_\infty \bar{T}_2/\delta$	$U_\infty \delta/\nu$ ($\times 10^{-5}$)	Mean dune height (m)	Boil observation (s)	Number boils counted
Lower Wabash River near Grayville, Illinois, U.S.A.									
14. ix. 1974	4·55	1·09	30·0	*	7·2	51·9	0·18	120	4
14. ix. 1974	3·60	1·08	19·0	13·0	5·6	39·6	0·20	600	32
14. ix. 1974	2·00	1·02	22·0	18·0	11·3	20·9	0·25	600	27
9. xi. 1974	0·55	0·64	5·9	n.d.	6·9	2·70	0·12	300	51
9. xi. 1974	1·00	0·80	9·8	6·0	7·9	6·19	0·15	600	61
9. xi. 1974	1·55	0·96	12·0	8·2	7·3	11·5	0·25	900	76
9. xi. 1974	2·75	1·12	17·0	11·0	7·0	24·0	0·23	1500	87
9. xi. 1974	5·20	1·42	35·0	32·0	9·6	58·6	0·23	1200	34
9. xi. 1974	4·75	1·10	36·0	31·0	8·4	42·1	0·14	1200	33
9. xi. 1974	3·70	1·31	16·0	15·0	5·7	40·1	Flat bed	1200	75
9. xi. 1974	5·60	1·50	29·0	29·0	7·7	69·1	0·34	1500	52
9. xi. 1974	2·00	0·97	18·0	17·0	8·9	16·1	0·22	900	49
9. xi. 1974	0·70	0·66	9·1	n.d.	8·6	3·83	0·12	600	66
9. xi. 1974	2·50	1·14	16·0	14·0	7·4	23·4	0·31	900	55
Arithmetic mean of above 14 values = 7·8									
Polomet' River, U.S.S.R. (Data from table 3 and figure 6 of Korchokha 1968)									
29. iv. 1963	0·70	0·88	9·9	?	12·5	4·1	0·30	?	?
25. iv. 1965	1·90	1·50	8·0	?	6·3	19·0	0·70	?	?
18. iv. 1966	1·70	1·10	10·0	?	6·5	12·5	0·45	?	?
28. iv. 1966	2·10	1·66	8·0	?	6·3	23·0	0·0?	?	?
Arithmetic mean of above 18 values = 7·8									
Arithmetic mean of above 18 values + 10 remaining values in Korchokha (1968, figure 6) = 7·6									

TABLE 1. Summary of boil measurements. Flow Reynolds numbers for Polomet' River estimated by assuming reasonable values for kinematic viscosity of water. Velocities for Polomet' River assumed to be those at free surface. σ is the standard deviation of boil periods; the other symbols are defined in the text.

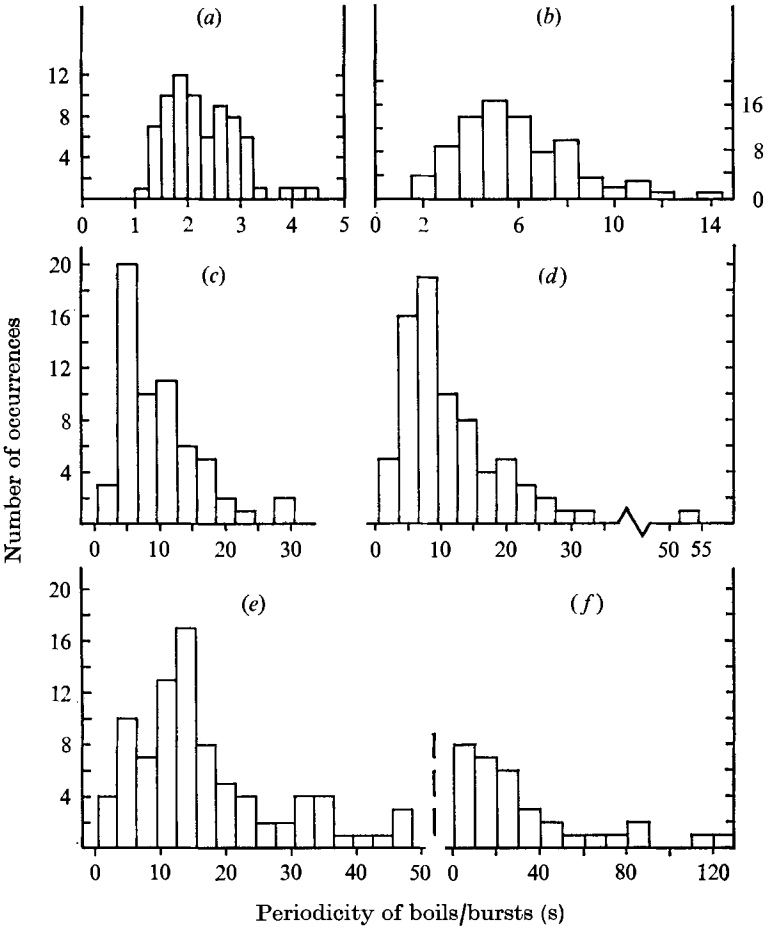

FIGURE 8. Histograms of boil periodicity T_2 in lower Wabash River [(c)–(f)] and of burst periodicity T_1 in laboratory flow of Kim *et al.* [(a), (b)] (1971, figures 21*b* and 22*b*). Table 1 summarizes boil measurements. (*a*) $\bar{T}_1 = 2{\cdot}3$ s, $\sigma = 0{\cdot}71$ s, $N = 73$. (*b*) $\bar{T}_1 = 6{\cdot}5$ s, $\sigma = 3$ s, $N = 87$. (*c*) $\bar{T}_2 = 9{\cdot}8$ s, $\sigma = 6{\cdot}0$ s, $N = 60$. (*d*) $\bar{T}_2 = 12$ s, $\sigma = 8{\cdot}2$ s, $N = 75$. (*e*) $\bar{T}_2 = 17$ s, $\sigma = 11$ s, $N = 86$. (*f*) $\bar{T}_2 = 35$ s, $\sigma = 32$ s, $N = 33$.

The slightly greater scaling constant of $7\frac{1}{2}$ in (5) compared with 5 in (4) can be explained readily. Many bursts and ejections in laboratory flows do not penetrate the boundary layer entirely. For example, Grass (1971, p. 253) mentioned the arrival of especially vigorous bursts of the water surface. Less energetic bursts presumably did not penetrate the water surface, which inference is consistent with $\bar{T}_2^* > \bar{T}_1^*$.

Figures 8 and 9 offer further support for the process described in figure 6. Histograms of boil periods resemble histograms of burst periods. Both sets of histograms show a consistent positive skewness, implying a tendency towards irregularly long periods between bursts and boils, and modal values appreciably less than means. When plotted on probability paper (not shown), the cumulative distribution of T_2 for each Wabash station fits a lognormal distribution fairly

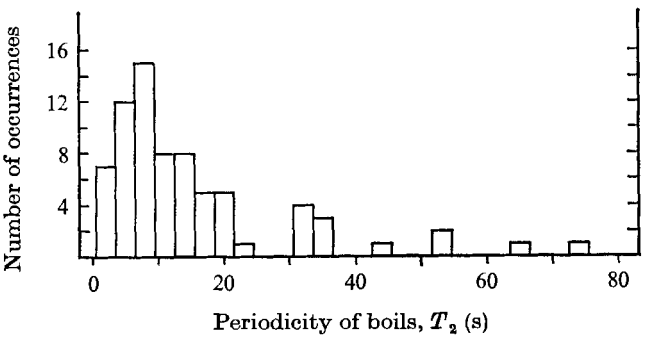

FIGURE 9. Histogram of boil periodicity over flat bed in lower Wabash River. Table 1 summarizes hydraulic data. $\bar{T}_2 = 16$ s, $\sigma = 15$ s, $N = 74$.

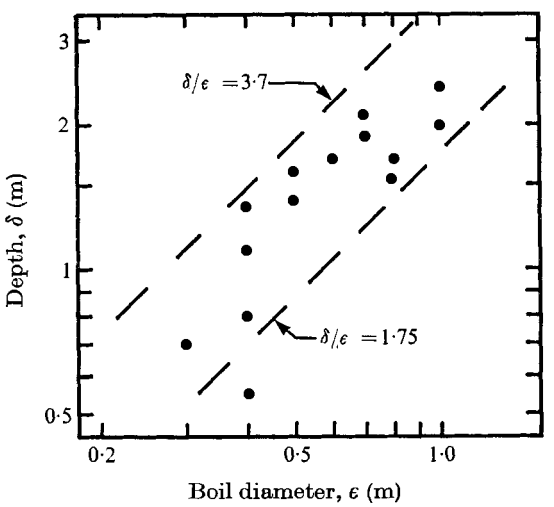

FIGURE 10. Boil diameter versus flow depth in Polomet' River, U.S.S.R. Dashed lines define bandwidth of 2·1. Data from Korchokha (1968, table 3).

well. Rao *et al.* (1971, p. 346) stated that burst periodicity T_1 was described best by this distribution.

Comparing figure 9 with figure 8 reveals a greater intermittency of boils over a flat bed than over rippled beds. The intermittency formed in the field as the second turbulent pattern described by Jackson (1975*a*, p. 242), an alternation of periods of boils with times of water-surface placidity. This macroturbulence phenomenon corresponds to type I(1) of Matthes (1947). It was detected in the deeper (greater than 3 m or so) flows over all bed roughnesses. A tendency towards increasing intermittency with depth or with boil periodicity exists in figure 8.

Korchokha's (1968) remarkable data on boils contain an additional item of interest. A plot of boil diameter versus flow depth (figure 10) discloses a rough proportionality, with all but one of 14 points lying within a 'bandwidth' of 2·1. This bandwidth appeared in the scaling relations for bursts (figure 3) and for boils (figure 7). If boils correspond to bursts, a proportionality of boil diameter

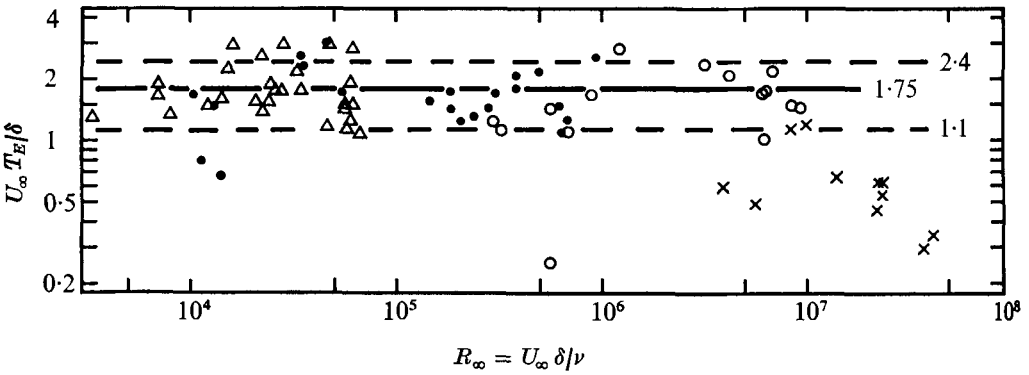

FIGURE 11. Scaling of Eulerian integral time scale with outer variables, emphasizing type of flow. ×, Mississippi River ($\delta > 6$ m); ○, canals and Missouri River (0·5 m $< \delta <$ 5 m); ●, flumes with moving bed material (0·04 m $< \delta <$ 0·60 m); △, flumes with no movement of bed material (0·02 m $< \delta <$ 0·29 m). 1·75 is arithmetic mean of T_E^* for all data except Mississippi River values. Dashed lines define bandwidth of 2·1, which includes most of the non-Mississippi data (cf. figures 3, 7, 10). Data from tables 1, 2, 4, 6–8, 10 and 11 of McQuivey (1973).

to flow depth would be expected from (4) and (5), because the product $U_\infty \overline{T}_i$, where $i = 1, 2$, defines a turbulent length scale (cf. Tennekes & Lumley 1972, pp. 9–17).

The above arguments suggest that bursts in natural open-channel flows appear as boils and kolks.

Inference of bursting from Eulerian integral time scale

The bursting process generally is thought to be the main turbulent structure in turbulent boundary layers (Grass 1971; Laufer 1975). There remains some uncertainty on the connexion between bursting and the large 'turbulent bulges' in the superlayer (Antonia 1972; Laufer 1975); but this problem vanishes in alluvial flows, where the boundary layer ordinarily is fully developed and encompasses the entire flow.

If the burst cycle is the main organized component of turbulence, then it should influence the various statistical macroscales of turbulence. The two relevant macroscales in this regard are the Eulerian integral time scale T_E and a derived length scale $L_x \equiv UT_E$ where U is the local mean velocity. In view of the organized structure of the burst cycle superimposed upon a background of unorganized 'random' turbulence, a direct relation between T_E and the mean duration of bursts $\overline{T}_{1B}$ seems appropriate. Any such correspondence would not depend upon the spatio-temporally random occurrence of bursts.

Only one connexion between T_E and burst periodicity has been suggested to date. Kim *et al.* (1971, p. 154) mentioned that the second mild maximum in the one-dimensional autocorrelation function $R(\tau)$ with time lag τ was very nearly the same as the $\overline{T}_1$ determined from simultaneous visual data. They cited only two comparisons and did not consider any possible relation between T_E and $\overline{T}_{1B}$.

McQuivey's (1973) exhaustive compilation of turbulence measurements in

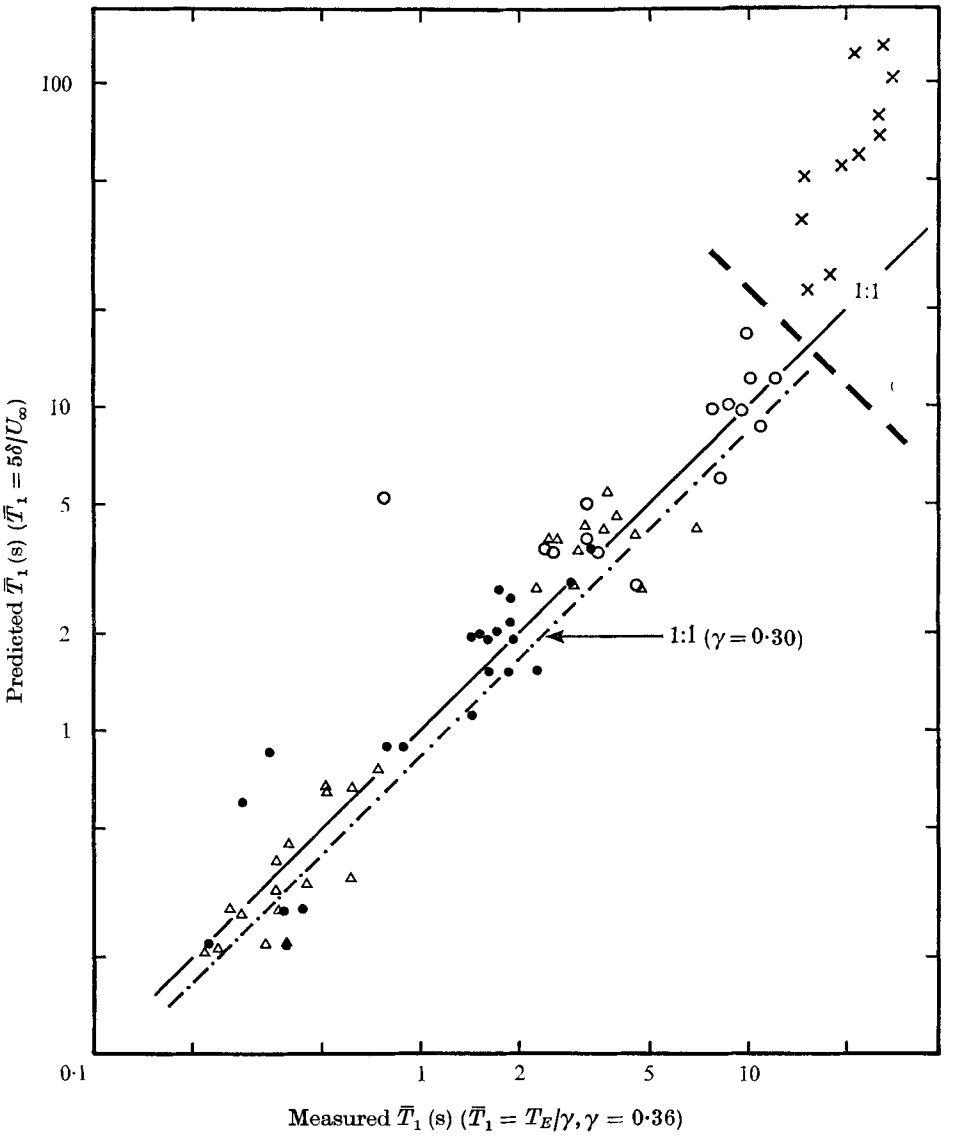

FIGURE 12. Comparison of predicted and measured values of mean periodicity of bursts. The measured values assume an apparent intermittency of 0·36. Data source is the same as for figure 11.

alluvial flows permits a test of the hypothesis that $T_E = \overline{T}_{1B}$. If they are proportional, they should have the same scaling. Unfortunately, the extreme difficulty in determining burst duration by probes or by visual methods in laboratory flows has prevented consideration of a scaling relation for $\overline{T}_{1B}$ like that for T_E in (4). However, there is no intrinsic reason why $\overline{T}_{1B}$ should scale differently; and from the scanty data on burst intermittency (Kim *et al.* 1971, figure 13; Brodkey *et al.* 1974, figure 4; Willmarth & Lu 1974, figures 12–15), one sees that the intermittency of bursts γ_1 is about 0·3 for non-dimensional distances

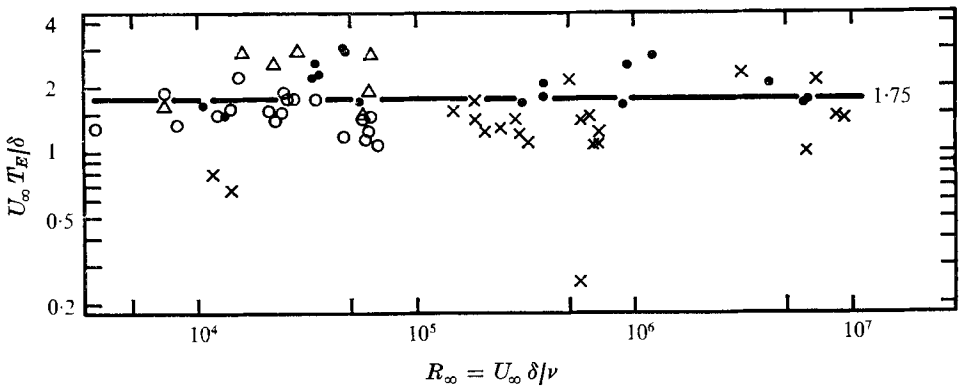

FIGURE 13. Scaling of Eulerian integral time scale with outer variables, emphasizing bed roughness. Symbols defined in table 2. The arithmetic mean of all data plotted is 1·75. The removal of three anomalously low values of T_E^* yields an arithmetic mean of 1·81, which corresponds to an apparent intermittency of 0·36. The data are the same as in figure 11, except for the removal of the Mississippi River measurements.

Bed roughness	Symbol in figure 13	Range in T_E^*	Mean T_E^*	Range in δ (m)	Number of data
The following data are incorporated in figure 13					
Smooth rigid bed	△	1·47 to 2·93	2·32	0·029 to 0·281	7
Lower-regime or upper-regime flat bed ($0{\cdot}1\,\text{mm} < d < 0{\cdot}4\,\text{mm}$)	●	1·48 to 3·01	2·11	0·041 to 4·97	18
Shot or rock roughness (immobile)†	○	1·07 to 2·22	1·52	0·020 to 0·288	19
Small scale ripples or dunes ($0{\cdot}2\,\text{mm} < d < 0{\cdot}5\,\text{mm}$)	×	0·251 to 2·32 1·00 to 2·32‡	1·30 1·42‡	0·037 to 4·75 0·283 to 4·75‡	21 18‡
The following data, from McQuivey's tables 3*a and* 3*b, are not in figure* 13					
0·32 cm block roughness		1·94 to 2·01	1·97	0·125 to 0·126	3
1·27 cm block roughness		1·22 to 2·75	1·97	0·125 to 0·132	11
2·86 cm block roughness		0·944 to 2·29	1·66	0·124 to 0·131	13

† Roughnesses were 0·439 cm lead shot, 1·9 cm rock, 3·8 cm rock and a mixture of 3·8 cm rock and 10–14 cm rock.

‡ Three lowest values of T_E^* removed.

TABLE 2. Summary of McQuivey's (1973) turbulence measurements.

above the bed $u_* y/\nu = y^+ > 50$. If so, then $\bar{T}_{1B}$, and presumably T_E, should scale according to (4), but with a constant of about 1·5. The plot of McQuivey's (1973) data in figure 11 demonstrates that T_E does scale like $\bar{T}_1$, with a scaling constant only slightly greater than the expected value. The following considerations will clarify this assertion.

The flow Reynolds number R_∞ appears in figure 11 instead of the momentum-thickness Reynolds number R_θ, which equals $U_\infty \theta/\nu$, where θ is the momentum

thickness of the boundary layer, used by the data sources of figure 3. The only justification for choosing R_θ lies in the more accurate measurement of θ in the developing flows in the laboratory. This advantage disappears in alluvial flows, where δ is merely the local flow depth. Over the range of Reynolds numbers in figures 3 and 11, $\theta \simeq \frac{1}{10}\delta$.

The Mississippi River data in figure 11 show comparatively low values of $U_\infty T_E/\delta$ ($\equiv T_E^*$), especially for $R_\infty > 10^7$. This apparent deviation from the anticipated trend is reconciled as follows. McQuivey (1973, p. B8) employed a constant sampling time of 4 min during the river measurements. As long as burst periods were much less than 4 min, sampling of a statistically adequate number of bursts was ensured. However, for the Mississippi measurements, $\overline{T}_1$ from (4) becomes of the order of 1 min, at which point the data begin to deviate from the trend (figure 12). Measured and predicted values of $\overline{T}_1$ in figure 12 agree well as long as predicted values do not exceed 20 s. Beyond this time limit, measured values become rather constant; this tendency may mean that 'eddies' of a time scale smaller than individual bursts have become the main contributors to T_E.

A third consideration in McQuivey's data is illustrated in figure 13, where the offending Mississippi values were removed to clarify the behaviour of T_E^* with bed roughness, an inner variable. None of the four roughness classes of figure 13 displays any apparent variation with R_∞, even though some rock roughnesses exceeded $\frac{1}{2}\delta$. T_E^* in figure 13 appears to be independent of mobility of bed material but tends to decrease with increasing bed roughness (table 2). However, artificial block roughnesses in table 2 show no discernible trend with T_E^*; their mean values are near the 1·75 grand mean of the natural roughnesses of figure 13. Figures 12 and 13 thus suggest that

$$U_\infty T_E/\delta \equiv R_E^* \simeq 1{\cdot}75 \tag{6}$$

is valid in a great variety of alluvial flows.

McQuivey (1973) computed T_E by integrating only over a lag time sufficient to bring $R(\tau)$ to zero. Kim *et al.* (1971, p. 154) pointed out that this practice means that longer-period turbulence phenomena will be missed entirely. Specifically, the second mild maximum in $R(\tau)$, which they found to correspond to $\overline{T}_1$, cannot be inferred. On the other hand, McQuivey's processing enhances any relationship between T_E and $\overline{T}_{1B}$, by effectively filtering out longer time scales.

In figure 13, 62 of the 65 values of T_E^* fall between 1 and 3. This bandwidth is only a little larger than the bandwidths of 2·1 in figures 3, 7 and 10 (cf. figure 11), which span much narrower ranges of R_∞.

To recapitulate, scaling relations in figures 11–13 support strongly the hypothesis that $T_E = \overline{T}_{1B}$.

5. Application of burst cycle to bedforms

Jackson (1975*b*) proposed three fundamental classes of bedforms produced by shearing flow and composed of cohesionless material. Two classes, microforms and mesoforms, are controlled directly by flow conditions in the turbulent boundary layer of the flow system. The controlling factor for microforms is

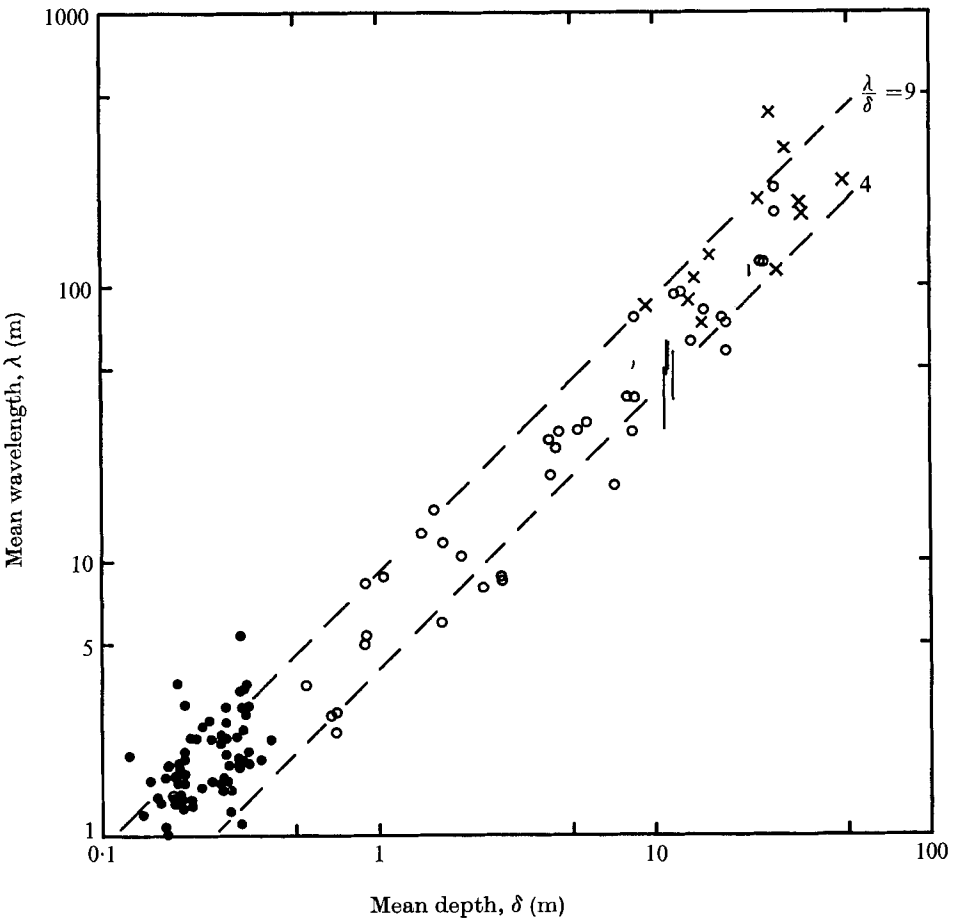

FIGURE 14. Group-mean wavelength of dunelike large-scale ripples versus mean depth in equilibrium open-channel aqueous flows. The minimum of five successive ripples was used to determine each value plotted. ●, flume; ○, rivers; ×, marine environments; |, Nasner's ranges. Table 3 lists sources of data. Stride's (1970) measurements of a train of 430 dunelike large-scale ripples in the North Sea are not shown; mean wavelengths (of 10 successive ripples at a time) in his figure 2 fall between 6 times and 10 times the corresponding mean depths (23 m to 33 m). Hypothesis $\lambda = U_\infty \overline{T}_2 \approx 7\delta$.

the turbulent structure of the inner zone. The fluid-dynamic regime of the outer zone governs mesoforms, with the bursting process exerting effective control in many flows.

Dunes

There is now abundant evidence that a large group of mesoforms, the dunelike large-scale ripples (dunes), are directly controlled by, and in turn control to some extent, the bursting process in the outer zone. An earlier section described the localization of bursts to ripple leesides. In spite of this apparent control by ripple morphology, boils over rippled beds scaled with outer variables in the same fashion as bursts. The direct influence of bursting upon dune morphology

Setting	Flow characteristics	Number of data	Reference	Range in mean δ (m)
	Flumes 78			
2·7 m wide flume	Steady uniform	78	Guy *et al.* (1966, tables 2–6, 10)	0·125 to 0·405
	Rivers 40			
Lower Wabash	Transiently steady quasi-uniform	14	This paper	0·90 to 8·5
Lower Mississippi	Transiently steady quasi-uniform	2	Anding (1970, figure 67)	13·7 to 18·3
Lower Mississippi	Transiently steady quasi-uniform	7	Lane & Eden (1940), cited in Jordan (1962, table 1)	8·5 to 27·4
Lower Mississippi	Slightly waning quasi-uniform	1	Carey & Keller (1957, figure 8)	27·5
Columbia	Low flow, quasi-uniform	1	Jordan (1962, figure 2)	11·9
Polomet', U.S.S.R.	Uniform, transiently steady	5	Korchokha (1968, table 3)	0·55 to 2·40
Polomet' and Volga, U.S.S.R.	Steady uniform low flow	3	Snischenko (1966, table 2)	0·184 to 5·70
Atrisco lateral canal	Steady uniform low flow	3	Nordin (1971, tables 1 and 3)†	0·671 to 0·701
Atrisco lateral canal	Steady uniform low flow	3	Culbertson, Scott & Bennett (1972, figures 12, 13, 16)	1·43 to 1·71
Parana	Steady quasi-uniform	1‡	Stückrath (1969, figure 4)	12·5
	Marine environments 12 + 5 *ranges*			
Delaware and San Francisco Bays	Tide-dominated estuarine	3	Jordan (1962, figure 2)	15·2 to 28
Southern Bight, North Sea	Tide-dominated with storm surges	2	McCave (1971, figures 5A–5B)	30 to 34
North Sea	Tide-dominated with storm surges	5	Van Veen (1935)	9·5 to 38
Outer Jade, North Sea	Tide-dominated estuarine channel	2	Reineck & Singh (1973, figure 48)	14 to 16
Outer Elbe, North Sea	Tide-dominated estuarine channel	1§	Nasner (1974, table 5)	22
Weser River, West Germany	Tidal estuary	4§	Nasner (1974, table 5)	10·9 to 11·6

† Other data from this source came from boundary layers which were not fully developed.

‡ 6 profiles show virtually identical mean wavelengths and mean depths. Single point plotted is arithmetic average of the mean wavelengths and mean depths.

§ Each datum is a range in mean wavelengths determined from repetitive depth profiles.

TABLE 3. Sources of data for figure 14. Transiently steady flow refers to stream discharge sufficiently constant for a long enough time before the profiling that the large-scale ripples should be in temporary equilibrium with the flow.

is suggested by the hypothesis of figure 14, which the following comments amplify further.

The belief that dunes are controlled by flow conditions in the entire boundary layer is not new. Kondrat'ev *et al.* (1959, pp. 28–37) suggested that dunes were generated by macroturbulence ('eddy formations') in the stream. Their description (pp. 37–39) of eddy formations in streams more than superficially resembles the bursting models summarized in figures 1 and 2. Kondrat'ev *et al.* concluded that periodicity of macroturbulence, when expressed as a wavelength, matched dune wavelengths. Yalin (1972, pp. 204–227) revived these concepts to propose a ratio of dune wavelength to depth in steady uniform flow equal to 2π. He concluded (pp. 243–246) that the proportionality improved as the grain Reynolds number $u_* d/\nu = R_g$ increased. The data of figure 14 follow Yalin's ratio well.

Not all flows display dunes in accordance with figure 14. Unsteady flows can introduce lag effects, in which mean-flow conditions change too rapidly for bedforms to adjust. In such cases, dune wavelength may bear no relation to depth, as in the extreme, but common, occurrence of dunes stranded and exposed by waning flow. Because hydraulic and morphological relationships for bedforms in steady uniform flows often become invalid in unsteady flows (Allen 1973, 1974; Allen & Collinson 1974) or in highly non-uniform flows (Jackson 1976), data in figure 14 were selected to minimize both complications. The river and flume data came from effectively steady flows which were uniform or nearly so (table 3). Marine data came from subtidal flows which were deep enough for the tidal range to be much less than the mean depth; bedforms consequently were in approximate equilibrium with the flow.

Data in figure 14 largely fall within a bandwidth of 2 and indicate an average wavelength-to-depth ratio of about 7 or 8. The length scale formed by the product of U_∞ and $\overline{T}_2$ is about 7·5 times δ (cf. figure 7 and (5)), in good agreement with the trend of figure 14. This fact and the previously noted observations of boils over flat beds bolster the hypothesis used in figure 14 and help justify the notion that bursting produces dunes.

Yalin (1972, pp. 226–227) argued that large transverse dunes in sand deserts form from the same macroturbulence phenomena as dunes in aqueous flows. Lack of meteorological data from deserts regrettably prevents a quantitative evaluation of this possibility.

Current lineations

Current lineations are alternating ridges and broad hollows, of a few grain diameters in relief and aligned parallel to the mean flow. Recent observations of their formation in aqueous flows suggest a close association with sublayer streaks. Williams & Kemp (1971, pp. 514–515) and Karcz (1973, pp. 161–163) described the segregation of sand grains moving over current-lineated beds into rectilinear stringers. Williams & Kemp (1971, p. 515) mentioned the formation of the ridges of current lineation by this process; they and Karcz (1973) nominated sublayer streaks for the controlling mechanism.

Allen (1968, pp. 32–33; 1970, figure 2·1) and Karcz (1973, figure 10) proposed the existence of organized helical flow in wall streaks to account for the grain

segregation necessary to form current lineations. Although sublayer streaks incorporate a weak streamwise vorticity (Kline *et al.* 1967, figures 10 and 13), the lateral component of flow within them is not nearly so rigidly structured as Allen and Karcz imply. An alternative mechanism comes from the observations of Williams & Kemp (1971, p. 515) and Karcz (1973, p. 161) for sand beds and of Allen (1964, p. 103) and Grass (1971, p. 250) for rigid smooth beds. All four papers reported alternating 'lanes' (parallel to mean flow) of faster-moving, clear fluid and of slow, sediment-laden fluid. The lanes were spaced in approximate agreement with (1). Karcz (1973, p. 163) mentioned that they were "affected by burst-induced steplike motions". These descriptions support the idea of low-speed wall streaks producing ridges and high-speed streaks being related to hollows. The fact that high-speed streaks preferentially suffer sweeps whereas low-speed streaks undergo lift-up also favours this scheme, in the following manner: to preserve continuity, fluid nearest the bed must be transported laterally from high-speed streaks to low-speed streaks, which would account for grain segregation into the latter. Because wall streaks are distributed randomly in space and in time over flat beds, the proposed mechanism is dynamic and rapidly changing. Once formed, however, the lineations probably fix the streaks to an appreciable degree.

Association of wall streaks with current lineations implies that the mean spacing of ridges should satisfy (1). While no published results are at hand to test this necessary condition, Allen's (1964) data on ridge spacing are entirely compatible with (1). Allen (1970, p. 69) pointed out that (1) restricts current lineations in aqueous flows to sediment of medium-sand size or finer. This prediction is obeyed in nature (Allen 1968, pp. 32–33). Sublayer disruption over rough beds imposes essentially the same upper bound on grain size.

Small-scale ripples in aqueous open-channel flows

A common microform in open-channel flows is the small-scale ripple, or current ripple (Allen 1968). Many hydraulic engineers and sedimentologists attribute small-scale ripples to the behaviour of the viscous sublayer (e.g. Sundborg 1956, pp. 209–211; Raudkivi 1963, p. 31; Williams & Kemp 1971, pp. 520–521; Yalin 1972, pp. 228–230, 258–260). An element of reasoning common to this consensus is abundant evidence of the absence of small-scale ripples on bed material coarser than a definite mean size. Upper size limits reported in the literature range from 0·6 mm (Chabert & Chauvin 1963) to 0·92 mm for the coarse ripple bed stage of Moss (1972). The size limit in a steady uniform flow of depth 7 cm has been fixed at about 0·7 mm (Southard & Boguchwal 1973, figure 5). Minimum grain Reynolds numbers for sediment entrainment, as determined from a Shields diagram (Graf 1971, p. 96), range from about 11 for 0·6 mm sand to about 24 for 0·92 mm sand. Such values imply bed roughnesses in the lower part of the hydraulically transitional range, in which grain roughness partially disrupts the sublayer.

Many visual experiments involving current lineations also dealt with the initiation of small-scale ripples on flat beds. Williams & Kemp (1971, pp. 515–517) and Karcz (1973, p. 163) observed that the existence of sublayer streaks is necessary in order to produce random pile-ups a few grain diameters in relief, which subsequently evolve by scour into incipient small-scale ripples. The

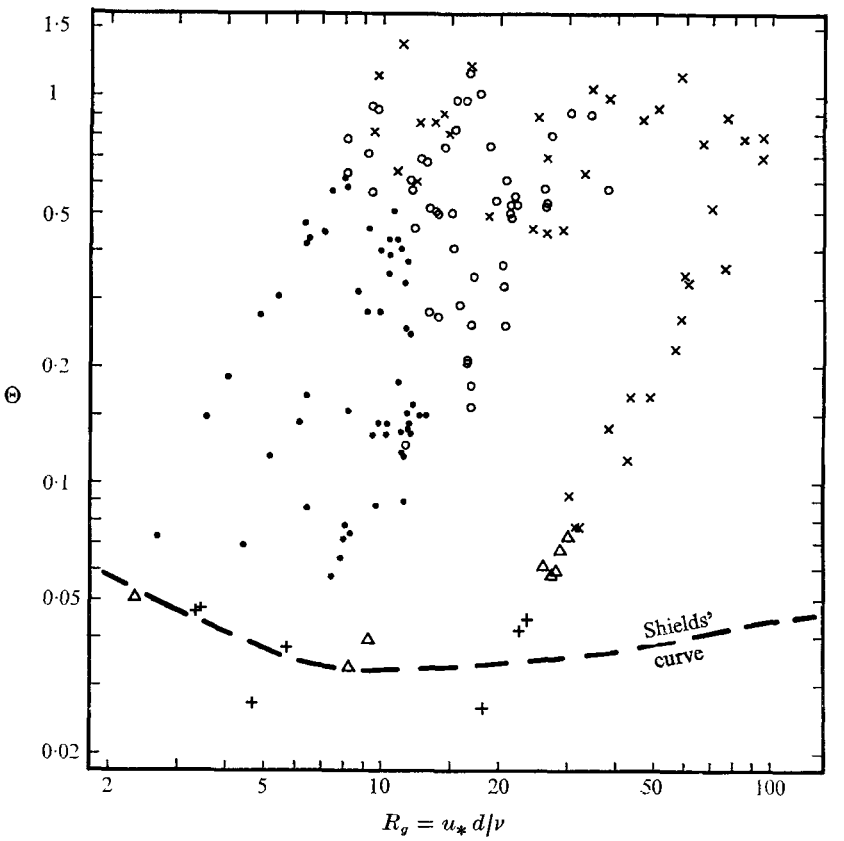

FIGURE 15. Existence fields of lower-regime bed configurations as a function of the dimensionless inner parameters Θ, the dimensionless shear stress (Bagnold 1966), and R_g (cf. similar plot in Allen 1970, figure 2.5). ×, dunes only; ○, dunes superimposed by small-scale ripples; ●, small-scale ripples only; △, lower plane bed with movement of bed material; +, plane bed with no movement of bed material. Data from Guy *et al.* (1966, tables 2–11). Only a representative sampling of the plane-bed data in Guy *et al.* is plotted. Shields' curve (heavy dashed line) is taken from Graf (1971, p. 96).

juvenile ripples then propagate additional ripples and, given sufficient sediment transport rates, eventually generate fully developed small-scale ripples (Southard & Dingler 1971; Williams & Kemp 1971).

If the generation of small-scale ripples depends upon wall streaks, then the ripples should not exist for grain Reynolds numbers beyond a certain value. The case for coarse sediment in which small-scale ripples never appear is evident: critical values of R_g for incipient motion are of the order of 10–20, or about twice the sublayer thickness. Flume data of Guy *et al.* (1966), when plotted on a Shields diagram (figure 15), show that small-scale ripples as a single bed phase do not exist when R_g exceeds 13. Small-scale ripples superimposed on the much larger dunes are restricted to grain Reynolds numbers between 8 and 40 (cf. Yalin 1972, pp. 232–234). Interpretation of the latter conclusion involves the non-uniform distribution of u_* (and hence R_g) over dunes, with near-zero or negative shear stresses in troughs and maxima at crests of individual dunes

(Raudkivi 1963, 1966; Smith 1969, figure 18; Smith 1970, figure 10). Because Guy *et al.* (1966) rarely described the locations of superposed ripples in enough detail to estimate the local u_*, this variability cannot be evaluated. However, most of their observations report superposed ripples in dune troughs or lower stress sides, where u_* tends to be much less than the channel mean incorporated in R_g in figure 15.

Graphs of the wavelength of small-scale ripples versus the flow depth in steady uniform flows (Allen 1970, figure 2.4; Yalin 1972, figure 7.27) show no discernible relationship between these two variables, in contrast to the marked proportionality for dunes (figure 14). On the other hand, dunes apparently incur no upper limits on R_g, which contains all three critical inner variables. For example, Baker (1973) has concluded that Pleistocene large-scale ripples of the Columbia scablands formed under typical conditions of $u_* = 1{\cdot}0$ m/s (see his table 2) and mean grain diameters of the order of 0·1 m, which yield values of R_g in the neighbourhood of 10^5. These considerations substantiate the concept of dunes as mesoforms and small-scale ripples as microforms.

The flume data of Guy *et al.* (1966) reveal that the spacing of small-scale ripples increases with u_*, which rules out a constant grain Reynolds number (the obvious candidate for scaling). Allen's (1970, figure 2.4) plot of the same data suggests an approximate inner scaling of

$$\lambda/d \simeq 1000 \text{ (small-scale ripples)}, \tag{7}$$

where d is the mean size of the bed material. Ratios of λ/d as low as 400 and as high as 3000 appear over the narrow range of grain sizes investigated (0·19–0·54 mm in mean size).

Textural differences in small-scale ripples

Enhancement of bursting over hydraulically transitional or rough beds (Grass 1971) may explain differences in bed-material texture between two types of small-scale ripples described by Moss (1972). A fine ripple bed stage appeared only in bed material finer than 0·25 mm in mean size; coarse ripple bed stages developed in sands of mean size 0·25–0·92 mm. Moss distinguished the two bed stages primarily by a much greater percentage of interstitial grains finer than 63 μm in the fine ripples. He attributed this textural disparity to the onset of 'microturbulence' between grains on the surface of coarse ripples, which swept out interstitial grains. Over the hydraulically smooth beds of fine ripples, grains would not protrude above the viscous sublayer and thus would not create microturbulence (Moss 1972, pp. 204–208).

Grass's (1971) measurements of turbulence intensity and descriptions of bursting over different bed roughnesses suggest the nature of Moss's microturbulence. Grass found an increase in the vertical intensity of turbulence with increasing bed roughness in a region of the turbulent boundary layer corresponding closely to the inner zone. His figure 5 shows a reduction of vertical intensity in this region of more than 50 % from a transitionally rough bed to a hydraulically smooth bed. Bagnold (1966, pp. I14–I16) deduced that the

maximum size of suspended sediment in flows of low sediment concentration is proportional to the root mean square of turbulent fluctuations in vertical velocity. These facts imply that Moss's microturbulence is in effect a significant increase in vertical turbulence intensity, due to more vigorous bursting. A suspension criterion to relate this notion explicitly to the textural difference could be calculated were it not for the well-documented variation (with R_∞) of vertical turbulence intensity over smooth beds (Clark 1968, figures 13 and 14). Grass (1971, p. 248) avoided this complication by maintaining R_∞ constant at about 6700 throughout his experiments, but his flow velocities fell below those necessary for incipient movement. However, the general trend of differences in turbulence intensity over beds of disparate roughness is probably preserved in natural flows.

6. Entrainment and suspension of sediment by bursts

In flows of low sediment concentration, the only means of suspending sediment not in contact with the bed is shear turbulence of the flow. Grain dispersive pressures (Bagnold 1966) and matrix strength (Fisher 1971; Hampton 1972) in such flows become ineffective agents of suspension and can be neglected. Southard (1971) determined lift forces not associated with turbulence also to be inadequate.

If one grants a dominant role to shear turbulence in sediment suspension, Bagnold's (1966, pp. I12–I14) argument for vertical anisotropy in shear turbulence becomes pertinent. He reasoned that vertically isotropic turbulence cannot suspend sediment, because the centre of gravity of the suspension will settle towards the boundary. Upward fluctuations in vertical fluid velocity must impart a greater momentum flux than downward fluctuations in order to suspend particles denser than the fluid. Preservation of continuity and of momentum then demands that upward fluctuations occur over a shorter time than downward fluctuations. This boundary condition thus requires a mechanism consisting of short-lived upward flow alternating with gentler return flow, longer in total duration, towards the bed.

A plausible candidate for the suspension mechanism is the bursting process. The following review of scattered observations on sediment dispersal from the bed presents qualitative support for this suggestion.

Observations of entrainment and concentration of sediment in kolks unanimously point towards the vertical anisotropy outlined above. Matthes (1947), Guy *et al.* (1966) and Korchokha (1968) described the upward transport of large amounts of sediment in kolks, with much material temporarily brought to the water surface in boils. The flows were ordinary lower-regime alluvial flows over dunes. In the Brahmaputra River, patterns of water-surface turbidity were generated by high sediment concentrations in boils (Coleman 1969, pp. 198–206). The turbidity contrast between boils and quiescent areas on the water surface allowed Coleman to map zones of boil development from aerial photographs. The author has observed fine and medium sand in concentrations of perhaps 1 % by weight in boils greater than 1 m in diameter in the lower Wabash River. Nearby temporarily placid areas of the water surface contained no sand.

Kolks apparently can erode quite large sedimentary particles from the bed in

	Inner zone	Outer zone
	Basic turbulent structure	
Extent	$y^+ \lesssim 50$	$y^+ \gtrsim 50$
Prevalent fluid motions	Wall streaks in viscous sublayer Lift-up stage of burst cycle	Oscillatory growth and breakup stages of burst cycle
Critical fluid-dynamic variables	u_*, d, ν (inner variables)	U_∞, δ (outer variables)
Scaling relations	$\lambda_s^+ \simeq 100$	$\bar{T}_1^* \simeq 5, \quad \gamma_1 \simeq 0{\cdot}3$
Relative contributions of bursts and sweeps to Reynolds stress	Sweeps predominate	Bursts predominate for $y^+ \gtrsim 100$
Effects of bed roughness	Grain roughness disrupts wall streaks when $d^+ \gtrsim 10$	Form roughness (esp. ripples) localizes generation of bursts to areas of adverse pressure gradients Grain roughness intensifies bursting
	Relation to other turbulent phenomena	
Boils and kolks	Lift-up initiates kolk Kolks preferentially form in areas of adverse pressure gradients	Kolk = Oscillatory growth stage Boil = Late oscillatory growth + breakup stages of burst cycle
Scaling relations of boils		$\bar{T}_2^* \simeq 7{\cdot}5, \quad \epsilon/\delta \simeq 0{\cdot}4$
Eulerian integral scale (T_E)		$T_E^* = \bar{T}_{1B}^* \simeq 1{\cdot}75$
	Relation to bedforms and sediment transport	
Bedforms (Jackson 1975*b*)	Microforms governed by turbulent structure of inner zone	Mesoforms governed by fluid-dynamic regime of outer zone
Scaling relations of bedforms	Current lineations: $\lambda^+ \simeq 100$ Small-scale ripples: $d^+ < 13$† Small-scale ripples: $\lambda/d \simeq 1000$	Dunelike large-scale ripples (Dunes): $\lambda \simeq 7\delta \simeq U_\infty \bar{T}_2$
Sediment dispersal	Wall streaks concentrate moving grains into low-speed wall streaks Grain roughness intensifies bursting to remove fine interstitial grains	Bursts produce vertical anisotropy in turbulence necessary to suspend sediment Vigorous upward flow in bursts entrains more and coarser sediment than tractive forces alone.

† For small-scale ripples superimposed on dunes, $8 < d^+ < 40$.

TABLE 4. Summary of bursting phenomenon in turbulent boundary layers of geophysical flows.

deep rivers, owing to the large lifting forces of the vortex motions. Matthes (1947) suggested that kolks could entrain coarse gravel. Tiffany (1963, pp. 58–65) summarized earlier measurements of pressure fluctuations on revetments in the lower Mississippi River; lift forces inferred from pressure fluctuations far exceeded the tractive force of the mean flow in ability to remove boulder-sized concrete slabs from the bed. Baker (1973) implicated kolks developed over boulder roughness as the agent responsible for plucking joint-bounded boulders from bedrock during catastrophic Pleistocene floods over the Columbia scablands.

A final indication of the major role of bursting in sediment dispersal is the novel visualization experiments of Velikanov & Mikhailova (1950). Their figure 2 shows sediment periodically thrown from the bed into the main part of the flow. Periods of these pulsations in sediment concentration appear to scale crudely

with figure 13 (see their figures 3 and 6). They also mentioned that the longitudinal correlation of fluid motions was nearly identical to that of sediment concentration.

Probe measurements (reviewed in the first part of § 4) suggest a markedly greater contribution to Reynolds stress from bursts than from sweeps in the zone $y^+ \gtrsim 100$ or $y/\delta \gtrsim 0{\cdot}05$. The prevalence of sweeps, which transport high-speed fluid towards the bed (Nychas *et al.* 1973), in the thin interval below this zone does not contradict the proposed effects of bursting upon sediment suspension. In this near-bed region, less than 1 cm thick in most natural flows, sediment-laden flows contain a 'heavy fluid layer' (Einstein & Chien 1955; Jopling (1965), which includes particles rolling or sliding on the bed and grains in intermittent suspension. Both modes of transport are much less dependent upon turbulence than is suspension. Bursts may merely tap this region of high sediment concentration to bring large amounts of sediment into the outer regions of the boundary layer. Or, if roughness elements are large enough to cause R_g to exceed the thickness of the inner zone, lifting forces induced by bursts may act directly upon the large bed particles to promote their entrainment.

The preceding remarks implicate bursting as the primary fluid-dynamic mechanism for suspension of sediment in low-concentration flows. They further suggest that bursts in deep alluvial flows play an essential role in the entrainment of large sedimentary particles.

7. Conclusions

The bursting phenomenon exists in turbulent boundary layers of all geophysical flows except perhaps (i) open-channel flows in the upper part of the upper flow regime and (ii) rapidly oscillating flows (wave boundary layers). Rough beds and entrained sediment may modify the intensity of bursting but do not alter the basic burst cycle. Bursting appears in flows which may be deep, unsteady, non-uniform and compressible.

Table 4 lists other major conclusions of this study.

Conversations with C. M. Gordon and T. J. Hanratty clarified several ideas developed in this paper. Critical reviews by R. S. Brodkey, A. L. Kistler and W. C. Krumbein improved an earlier version of the manuscript. The Department of Geology, University of Illinois at Urbana-Champaign, provided field equipment for hydraulic measurements in the lower Wabash River.

REFERENCES

Allen, J. R. L. 1964 Primary current lineation in the Lower Old Red Sandstone (Devonian), Anglo-Welsh Basin. *Sedimentology*, **3**, 89–108.

Allen, J. R. L. 1968 *Current Ripples.* North-Holland.

Allen, J. R. L. 1970 *Physical Processes of Sedimentation.* Elsevier.

Allen, J. R. L. 1973 Phase differences between bed configuration and flow in natural environments, and their geological relevance. *Sedimentology*, **20**, 323–329.

Allen, J. R. L. 1974 Reaction, relaxation, and lag in natural sedimentary systems: general principles, examples and lessons. *Earth-Sci. Rev.* **10**, 263–342.

ALLEN, J. R. L. & COLLINSON, J. D. 1974 The superimposition and classification of dunes formed by unidirectional aqueous flows. *Sediment. Geol.* **12**, 169–178.

ANDING, M. G. 1970 Hydraulic characteristics of Mississippi River channels. *U.S. Army Corps Engrs. Vicksburg, Miss., Potamology Investigations Rep.* no. 19–3.

ANTONIA, R. A. 1972 Conditionally sampled measurements near the outer edge of a turbulent boundary layer. *J. Fluid Mech.* **56**, 1–18.

BAGNOLD, R. A. 1956 The flow of cohesionless grains in fluids. *Phil. Trans.* A **249**, 235–297.

BAGNOLD, R. A. 1966 An approach to the sediment transport problem from general physics. *U.S. Geol. Surv. Prof. Paper*, no. 422-I.

BAGNOLD, R. A. 1973 The nature of saltation and of 'bed-load' transport in water. *Proc. Roy. Soc.* A **332**, 473–504.

BAKER, V. R. 1973 Erosional forms and processes for the catastrophic Pleistocene Missoula floods in eastern Washington. In *Fluvial Geomorphology* (ed. M. Morisawa), pp. 123–148. State University of New York, Binghamton.

BLINCO, P. H. & SIMONS, D. B. 1975 Turbulent structure near smooth boundary. *Proc. A.S.C.E., J. Engng. Mech. Div.* **101**, 241–255.

BOWDEN, K. F. 1962 Measurements of turbulence near the sea bed in a tidal current. *J. Geophys. Res.* **67**, 3181–3186.

BRODKEY, R. S., WALLACE, J. M. & ECKELMANN, H. 1974 Some properties of truncated turbulence signals in bounded shear flows. *J. Fluid Mech.* **63**, 209–224.

CAREY, W. C. & KELLER, M. D. 1957 Systematic changes in the beds of alluvial rivers. *Proc. A.S.C.E., J. Hydraul. Div.* **83** (HY4), 1331.

CHABERT, J. & CHAUVIN, J. L. 1963 Formation des dunes et des ridges dans les modèles fluviaux. *Bull. Centre Rech. et d'Essais Chatou*, no. 4.

CLARK, J. A. 1968 A study of incompressible turbulent boundary layers in channel flow. *J. Basic Engng*, D **90**, 455–468.

CLEMENS, S. (MARK TWAIN) 1896 *Life on the Mississippi*. Harper & Row.

COLEMAN, J. M. 1969 Brahmaputra River: channel processes and sedimentation. *Sediment. Geol.* **3**, 129–239.

CORINO, E. R. & BRODKEY, R. S. 1969 A visual investigation of the wall region in turbulent flow. *J. Fluid Mech.* **37**, 1–30.

CULBERTSON, J. K., SCOTT, C. H. & BENNETT, J. P. 1972 Summary of alluvial channel data from Rio Grande conveyance channel, New Mexico, 1965–1969. *U.S. Geol. Surv. Prof. Paper* 562-J.

EINSTEIN, H. A. & CHIEN, N. 1955 Effects of heavy sediment concentration near the bed on velocity and sediment distribution. *U.S. Army Corps Engrs, Missouri River Div., Rep. Sediment Ser.* no. 8.

FISHER, R. V. 1971 Features of coarse-grained, high-concentration fluids and their deposits. *J. Sedim. Petrol.* **41**, 916–927.

GORDON, C. M. 1974 Intermittent momentum transport in a geophysical boundary layer *Nature*, **248**, 392–394.

GORDON, C. M. 1975*a* Period between bursts at high Reynolds number. *Phys. Fluids*, **18**, 141–143.

GORDON, C. M. 1975*b* Sediment entrainment and suspension in a turbulent tidal flow. *Mar. Geol.* **18**, M57-M64.

GRAF, W. H. 1971 *Hydraulics of Sediment Transport*. McGraw-Hill.

GRASS, A. J. 1971 Structural features of turbulent flow over smooth and rough boundaries. *J. Fluid Mech.* **50**, 233–255.

GUPTA, A. K., LAUFER, J. L. & KAPLAN, R. E. 1971 Spatial structure in the viscous sublayer. *J. Fluid Mech.* **50**, 493–512.

GUY, H. P., SIMONS, D. B. & RICHARDSON, E. V. 1966 Summary of alluvial channel data from flume experiments, 1956–1961. *U.S. Geol. Surv. Prof. Paper*, no. 462-I.

HAMPTON, M. A. 1972 The role of subaqueous debris flow in generating turbidity currents. *J. Sedim. Petrol.* **42**, 775–793.

HAUGEN, D. A., KAIMAL, J. C. & BRADLEY, E. F. 1971 An experimental study of Reynolds stress and heat flux in the atmospheric surface layer. *Quart. J. Roy. Met. Soc.* **97**, 168–180.

HEATHERSHAW, A. D. 1974 'Bursting' phenomena in the sea. *Nature*, **248**, 394–395.

JACKSON, R. G. 1975*a* A depositional model of point bars in the lower Wabash River. Ph.D. dissertation, Illinois University, Urbana.

JACKSON, R. G. 1975*b* Hierarchial attributes and a unifying model of bedforms composed of cohesionless material and produced by shearing flow. *Bull. Geol. Soc. Am.* **86**, 1523–1533.

JACKSON, R. G. 1976 Largescale ripples of the lower Wabash River. *Sedimentology* (in Press).

JOPLING, A. V. 1965 Laboratory study of the distribution of grain sizes in cross-bedded deposits. In *Primary Sedimentary Structures and their Hydrodynamic Interpretation* (ed. G. V. Middleton), pp. 53–65. Soc. Econ. Paleontologists and Mineralogists, Spec. Publ. no. 12.

JORDAN, G. F. 1962 Large submarine sand waves. *Science*, **136**, 839–848.

KAIMAL, J. C. & BUSINGER, J. A. 1970 Case studies of a convective plume and a dust devil. *J. Appl. Met.* **9**, 612–620.

KARCZ, I. 1973 Reflections on the origin of some small-scale longitudinal streambed scours. In *Fluvial Geomorphology* (ed. M. Morisawa), pp. 149–173. State University of New York, Binghamton.

KIM, H. T., KLINE, S. J. & REYNOLDS, W. C. 1971 The production of turbulence near a smooth wall in a turbulent boundary layer. *J. Fluid Mech.* **50**, 133–160.

KLINE, S. J., REYNOLDS, W. C., SCHRAUB, F. A. & RUNDSTADLER, P. W. 1967 The structure of turbulent boundary layers. *J. Fluid Mech.* **30**, 741–773.

KOMAR, P. D. & MILLER, M. C. 1973 The threshold of sediment movement under oscillatory water waves. *J. Sedim. Petrol.* **43**, 1101–1110.

KONDRAT'EV, N. E., LYAPIN, A. N., POPOV, I. V., PIN'KOVSKII, S. I., FEDOROV, N. N. & YAKUNIN, I. I. 1959 *Channel Processes.* Leningrad: Gidrometeoizdat.

KORCHOKHA, YU. M. 1968 Investigation of the dune movement of sediments on the Polomet' River. *Sov. Hydrol.* pp. 541–559.

LANE, E. W. & EDEN, E. W. 1940 Sand waves in the lower Mississippi River. *J. Western Soc. Engrs*, **45**, 281–291.

LATHAM, D. J. & MIKSAD, R. W. 1974 Electric field perturbations of the marine atmosphere by horizontal roll vortices. *J. Geophys. Res.* **79**, 5592–5597.

LAUFER, J. 1954 The structure of turbulence in fully developed pipe flow. *N. A.C.A. Rep.* no. 1174.

LAUFER, J. 1975 New trends in experimental turbulence research. *Ann. Rev. Fluid Mech.* **7**, 307–326.

LAUFER, J. & BADRI NARAYANAN, M. A. 1971 Mean period of the turbulent production mechanism in a boundary layer. *Phys. Fluids*, **14**, 182–183.

LU, S. S. & WILLMARTH, W. W. 1973 Measurements of the structure of the Reynolds stress in a turbulent boundary layer. *J. Fluid Mech.* **60**, 481–511.

MCCAVE, I. N. 1971 Sand waves in the North Sea off the coast of Holland. *Mar. Geol.* **10**, 199–225.

MCQUIVEY, R. S. 1973 Summary of turbulence data from rivers, conveyance channels, and laboratory flumes. *U.S. Geol. Surv. Prof. Paper*, no. 802-B.

MARKSON, R. 1975 Atmospheric electrical detection of organized convection. *Science*, **188**, 1171–1177.

MATTHES, G. H. 1947 Macroturbulence in natural stream flow. *Trans. Am. Geophys. Un.* **28**, 255–262.

MERCERET, F. J. 1972 *An Experimental Study of Wind Velocity Profiles over a Wavy Surface.* College of Maritime Studies, Delaware University, publ. 2MS065.

MOLLO-CHRISTENSEN, E. L. 1973 Intermittency in large-scale turbulent flows. *Ann. Rev. Fluid Mech.* **5**, 101–118.

MONIN, A. S. 1970 The atmospheric boundary layer. *Ann. Rev. Fluid Mech.* **2**, 225–250.

MOSS, A. J. 1972 Bed-load sediments. *Sedimentology*, **18**, 159–220.

NASNER, H. 1974 Über das Verhalten von Transpörtkorpern im Tidegebiet. *Mitt. Franzius-Inst.* **40**, 1–149.

NORDIN, C. F. 1971 Statistical properties of dune profiles. *U.S. Geol. Surv. Prof. Paper*, no. 562-F.

NYCHAS, S. G., HERSHEY, H. C. & BRODKEY, R. S. 1973 A visual study of turbulent shear flow. *J. Fluid Mech.* **61**, 513–540.

OFFEN, G. R. & KLINE, S. J. 1973 Experiments on the velocity characteristics of 'bursts' and on the interactions between the inner and outer regions of a turbulent boundary layer. *Thermosci. Div., Mech. Engng Dept., Stanford Univ. Rep.* no. MD-31.

OFFEN, G. R. & KLINE, S. J. 1974 Combined dye-streak and hydrogen-bubble visual observations of a turbulent boundary layer. *J. Fluid Mech.* **62**, 223–239.

OFFEN, G. R. & KLINE, S. J. 1975 A proposed model of the bursting process in turbulent boundary layers. *J. Fluid Mech.* **70**, 209–228.

PANOFSKY, H. A. 1974 The atmospheric boundary layer below 150 metres. *Ann. Rev. Fluid Mech.* **6**, 147–177.

RAO, K. N., NARASIMHA, R. & BADRI NARAYANAN, M.A. 1971 The 'bursting' phenomenon in a turbulent boundary layer. *J. Fluid Mech.* **48**, 339–352.

RAUDKIVI, A. J. 1963 Study of sediment ripple formation. *Proc. A.S.C.E., J. Hydraul. Div.* **89** (HY6), 15–33.

RAUDKIVI, A. J. 1966 Bed forms in alluvial channels. *J. Fluid Mech.* **26**, 507–514.

REINECK, H.-E. & SINGH, I. B. 1973 *Depositional Sedimentary Environments.* Springer.

SCHLICHTING, H. 1968 *Boundary-Layer Theory.* McGraw-Hill.

SIMONS, D. B., RICHARDSON, E. V. & NORDIN, C. F. 1965 Sedimentary structures generated by flow in alluvial channels. In *Primary Sedimentary Structures and Their Hydrodynamic Interpretation* (ed. G. V. Middleton), pp. 34–52. Soc. Econ. Paleontologists and Mineralogists, Spec. Publ. no. 12.

SLEATH, J. F. A. 1970 Velocity measurements close to the bed in a wave tank. *J. Fluid Mech.* **42**, 111–123.

SLEATH, J. F. A. 1974*a* Stability of laminar flow at seabed. *Proc. A.S.C.E., J. Waterways, Harbors Coastal Engng Div.* **100**, 105–122.

SLEATH, J. F. A. 1974*b* Velocities above bed in oscillatory flow. *Proc. A.S.C.E., J. Waterways, Harbors Coastal Engng Div.* **100**, 287–304.

SMITH, J. D. 1969 Studies of nonuniform boundary-layer flows. In *Investigations of Turbulent Boundary Layers and Sediment-Transport Phenomena as Related to Shallow Marine Environments.* Oceanography Dept., Washington University, Seattle, Rep. no. A69-7.

SMITH, J. D. 1970 Stability of a sand bed subjected to a shear flow of low Froude number. *J. Geophys. Res.* **75**, 5928–5940.

SNISCHENKO, B. F. 1966 Movement of sand dunes in natural streams. *Sov. Hydrol.* pp. 486–493.

SOUTHARD, J. B. 1971 Lift forces on suspended sediment particles in laminar flow: experiments and sedimentological interpretation. *J. Sedim. Petrol.* **41**, 320–323.

SOUTHARD, J. B. & BOGUCHWAL, L. A. 1973 Flume experiments on the transition from ripples to lower flat bed with increasing sand size. *J. Sedim. Petrol.* **43**, 1114–1121.

SOUTHARD, J. B. & DINGLER, J. R. 1971 Flume study of ripple propagation behind mounds of flat sand beds. *Sedimentology*, **16**, 257–263.

STRIDE, A. H. 1970 Shape and size trends for sand waves in a depositional zone of the North Sea. *Geol. Mag.* **107**, 469–477.

STÜCKRATH, T. 1969 Die Bewegung von Großriffeln an der Sohl des Rio Paraná. *Mitt. Franzius-Inst.* **32**, 266–293.

SUNDBORG, A. 1956 The River Klarälven: a study of fluvial processes. *Geog. Annaler*, **38**, 125–316.

TELEKI, P. G. 1972 Wave boundary layers and their relation to sediment transport. In *Shelf Sediment Transport: Process and Pattern* (ed. D. J. P. Swift, D. B. Duane & O. H. Pilkey), pp. 21–59. Dowden, Hutchinson, and Ross, Stroudsburg, Pa.

TENNEKES, H. & LUMLEY, J. L. 1972 *A First Course in Turbulence.* MIT Press, Cambridge, Mass.

TIFFANY, J. B. 1963 Review of research on channel stabilization of the Mississippi River 1931–1962. *Channel Stabilization Comm., U.S. Army Corps Engrs, Vicksburg, Miss., Tech. Rep.* no. 2.

VANONI, V. A. & HWANG, L.-S. 1967 Relation between bed forms and friction in streams. *Proc. A.S.C.E., J. Hydraul. Div.* **93** (HY3), 121–144.

VAN VEEN, J. 1935 Sand waves in the North Sea. *Hydrograph Rev.* **12**, 21–29.

VELIKANOV, M. A. & MIKHAILOVA, N. A. 1950 The effect of large-scale turbulence on pulsations of suspended sediment concentration. *Acad. Sci. USSR Proc., Geogr. Geophys. Ser.* **14**, 421–424.

WALLACE, J. M., ECKELMANN, H. & BRODKEY, R. S. 1972 The wall region in turbulent shear flow. *J. Fluid Mech.* **54**, 39–48.

WILLIAMS, P. B. & KEMP, P. H. 1971 Initiation of ripples on flat sediment beds. *Proc. A.S.C.E., J. Hydraul. Div.* **97**, 505–522.

WILLMARTH, W. W. & LU, S. S. 1972 Structure of the Reynolds stress near the wall. *J. Fluid Mech.* **55**, 65–92.

WILLMARTH, W. W. & LU, S. S. 1974 Structure of the Reynolds stress and the occurrence of bursts in the turbulent boundary layer. In *Turbulent Diffusion in Environmental Pollution* (ed. F. N. Frenkiel & R. E. Munn), pp. 287–314. *Advances in Geophysics*, vol. 18A.

YALIN, M. S. 1972 *Mechanics of Sediment Transport.* Pergamon.

ZNAMENSKAYA, N. S. 1963 Experimental study of the dune movement of sediment. *Sov. Hydrol.* pp 253–275.

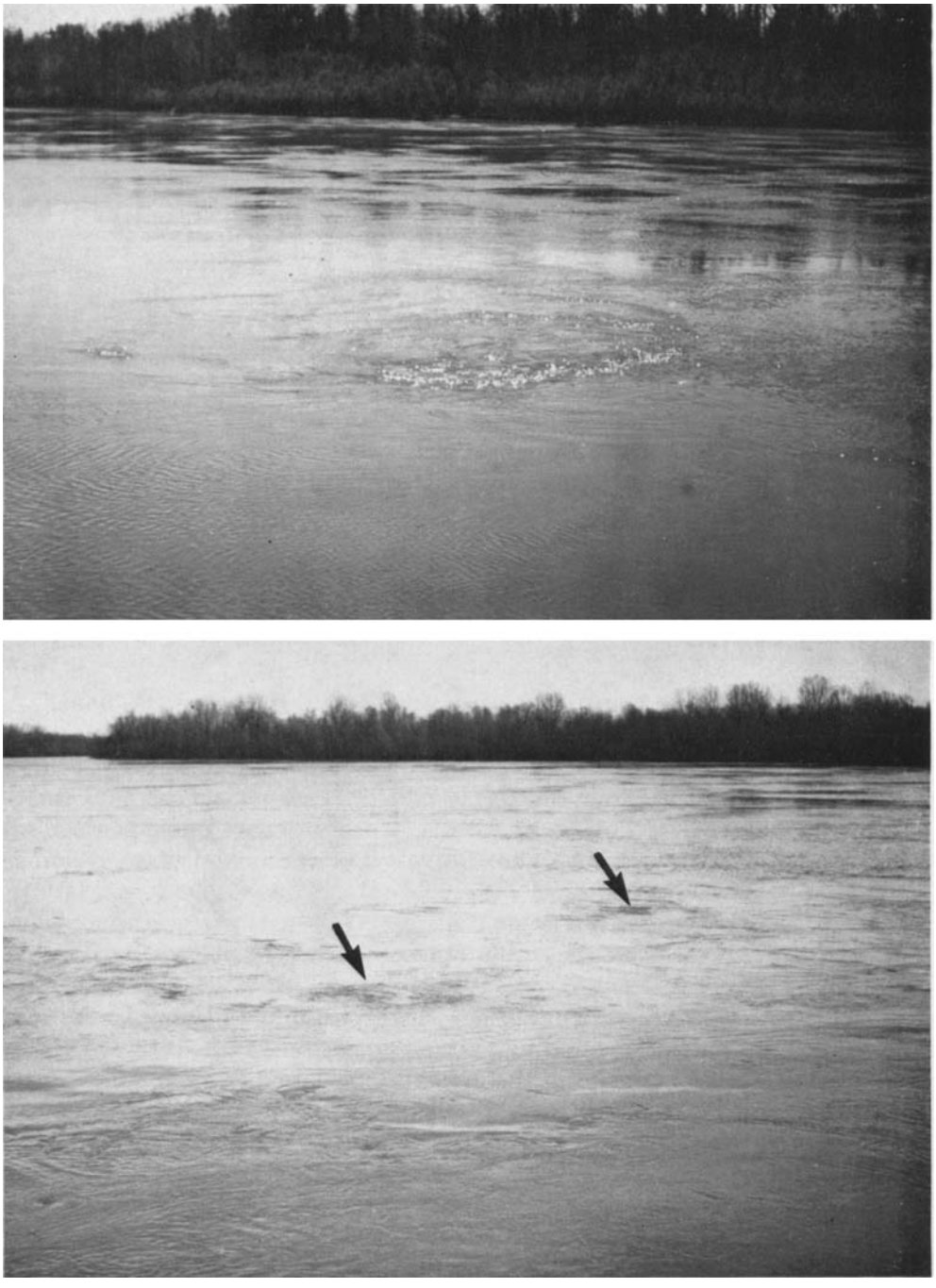

FIGURE 5. Boils in lower Wabash River. The growing boil in the centre of the upper photograph is about 1 m in diameter and outlined by white spots of reflected sunlight. The arrows in the lower photograph point to boils on the water surface which lie about 10 m downstream from the crest of a 1 m high transverse bar (water depth about 5 m). The two boils are about 1 m in diameter.